UDC 623.482:004.932.4

Ivannikov K. V., Gavrilov A. V., Boev A. S., Shoshin I. S.

Method of landing UAV of helicopter type using an infrared camera

The paper proposes using an infrared camera to detect the figure of a set of infrared emitters – guidance on the landing field. We developed an infrared guidance recognition algorithm and did its bench-test. Moreover, we made a program complex for modeling the landing field recognition during the landing of unmanned aerial vehicle (UAV) of helicopter type.

Keywords: landing, UAV, helicopter, infrared camera.

Introduction

In recent years, there has been a growing interest in the use of helicopter-type UAVs for military applications. Such aerial vehicles are able to carry various payload such as electronic countermeasures and electronic warfare systems, radars, target hit indicators when UAVs are used as aerial targets.

Landing is the most difficult and critical phase of the UAV flight. At this flight phase, there is no option to fully rely on satellite navigation systems, because satellite data are not sufficiency accurate and reliable, while multiple locations have no satellite coverage at all.

Infrared camera

We propose an infrared (IR) camera to be used as part of a landing zone recognition system, and, respectively, infrared radiation sources to be used as landing zone markers. An IR camera has the following advantage over a camera shooting in the visible range: it allows to obtain less segmented images that ease recognition of landing zone markers if there is no blocking IR radiation [1].

As a rule, one or more IR radiation sources are used as landing zone markers in case of IR camera application. There are two ways to separate interference from IR radiation sources during recognition: radiation simulation at a certain carrier frequency or making a primitive geometrical figure from a set of sources. *T*-shape and *H*-shape can be singled out as the most widely used figures. In this paper, we refer to the *T*-shaped figure, which due to its shape allows to specify the direction and use this information for adjusting the landing trajectory.

Recognition algorithm

We developed the recognition algorithm considering the requirement for the algorithm execution time that should not exceed 0.03 s when running on *Intel Core i*5 CPUs, taking into account that most modern IR cameras operate at a framerate of 30 fps.

Main algorithm stages:

- Gaussian smoothing;
- image binarization;
- morphological closing;
- identification of segment contours;
- marker detection.

Below we will analyse each algorithm stage in detail.

Gaussian smoothing. The first stage is intended for image processing using a smoothing filter based on the Gaussian function for the two-dimensional formulation:

$$G(x,y)=\frac{1}{2\pi\sigma^2}\times e^{-\frac{x^2+y^2}{2\sigma^2}},$$

where x – distance from the coordinate origin along the horizontal axis;

y – distance from the coordinate origin along the vertical axis;

σ – Gaussian distribution root-mean-square deviation.

Filtering improves the recognition quality by reducing the algorithm’s noise susceptibility. Smoothing has a positive effect upon the process of boundary detection, reduces the amount of false contours and improves the accuracy of identification of detected boundaries.

Image binarization. The next stage is intended to obtain a monochromatic image which has dark and bright pixels only. The key characteristic of the process is the brightness threshold allowing for such a transformation. The brightness threshold can be selected based on certain principles (binarization criteria). In this study, we applied the Otsu's method [2]. The method is based on classifying pixels into classes, foreground and background, in such a way that the intraclass dispersion is minimal. The interclass dispersion is calculated as the weighted sum of dispersions of two classes [2]:

$$\sigma_w^2(T) = n_1(T)\sigma_1^2(T) + n_2(T)\sigma_2^2(T),$$

where weights $n_1(T)$ and $n_2(T)$ are probabilities of two classes separated by threshold T;

$\sigma_1^2(T)$ and $\sigma_2^2(T)$ – dispersions of classes.

Morphological closing. In comparison with the algorithms represented, for example, in [1, 3], the distinctive feature of this algorithm is that it allows to recognize not a continuous contour of the landing zone marker's shape shown in the frame, but a contour made of individual segments corresponding to individual IR radiation sources.

For this reason, before the recognition procedure, we shall perform the mathematical operation of morphological closing [4] intended to merge individual segments shown in an image in order to form the contour of the landing zone marker's outline (for this example, we used the structure consisting of diodes emitting in the visible range) (Fig. 1).

The specific feature of morphological closing is the presence of a structure-forming element [1], the size of which affects the quality of contour merging. Since sizes of diodes and distances between them increase as the UAV flight altitude is becoming lower during landing, the size of the element is the monotonically increasing function of altitude in the algorithm.

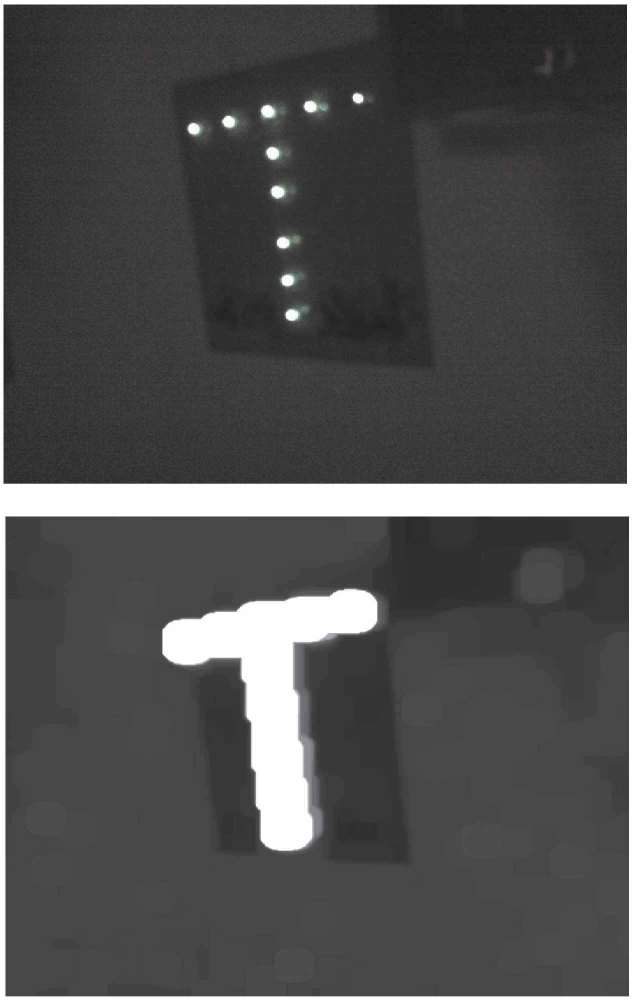

Fig. 1. Result of morphological closing represented by the *T* letter consisting of individual diodes

Identification of segment contours. After the morphological closing operation is completed, contours of segments shown in the image shall be found, and then the descriptors of the contour of each segment found shall be compared with nominal pre-calculated descriptors of the landing zone marker's outline.

Like the algorithm described in [1], we use the first four affine invariants of moments [5] that allow to identify the contour irrespective of the turning angle, size and position in the image. According to [5], affine invariants can be used in many cases as approximation of projection invariant for identifying 3D figures. Also, affine invariants allow to drastically reduce the amount of recognition errors in comparison with invariants *Hu* [4], which are often employed for identifying image contours [5]:

$$I_1 = \frac{m_{20}m_{02} - m_{11}^2}{m_{00}^4};$$

$$I_2 = (-m_{30}^2 m_{03}^2 + 6m_{30}m_{21}m_{12}m_{03} - 4m_{30}m_{12}^3 - 4m_{21}^3 m_{03} + 3m_{21}^2 m_{12}^2) / m_{00}^{10};$$

$$I_3 = \left(m_{20}(m_{21}m_{03} - m_{12}^2) - m_{11}(m_{30}m_{03} - m_{21}m_{12}) + m_{02}(m_{30}m_{12} - m_{21}^2)\right) / m_{00}^7;$$

$$I_4 = (m_{20}^3 m_{03}^2 - 6m_{20}^2 m_{11}m_{12}m_{03} - 6m_{20}^2 m_{02}m_{21}m_{03} + 9m_{20}^2 m_{02}m_{12}^2 + 12m_{20}m_{11}^2 m_{21}m_{03} + 6m_{20}m_{11}m_{02}m_{30}m_{03} - 18m_{20}m_{11}m_{02}m_{21}m_{12} - 8m_{11}^3 m_{30}m_{03} - 6m_{20}m_{02}^2 m_{30}m_{12} + 9m_{20}m_{02}^2 m_{21}^2 + 12m_{11}^2 m_{02}m_{30}m_{12} - 6m_{11}m_{02}^2 m_{30}m_{21} + m_{02}^3 m_{30}^2) / m_{00}^7,$$

where m_{pq} – central image moments.

For black and white image G, the central moments are calculated by the following formula:

$$m_{pq} = \sum_i \sum_j (x_i - x_c)^p (y_j - y_c)^q,$$

where (x_c, y_c) – image G centre coordinates.

Using central moments, we can also calculate angle θ between the main axis of the marker contour and X-axis of the coordinate system:

$$\theta = \frac{1}{2}\operatorname{arctg}\left(\frac{2m_{11}}{(m_{20} - m_{02})}\right).$$

If we know angle θ, we can minimize the course deviation.

Marker detection. A landing zone marker is supposed to be detected if the difference between the descriptors of the nominal contour and the descriptor of one of the contours found in the image is less than 0.0025. This figure is experimentally selected for a particular case.

The difference between descriptors is calculated by the following formula:

$$\text{dis} = \frac{\text{dif}}{\text{norm}};$$

$$\text{dif} = \sum_{i=1,4} \text{abs}\left(\frac{1}{\log(\mathbf{I}_i^H)} - \frac{1}{\log(\mathbf{I}_i)}\right);$$

$$\text{norm} = \sum_{i=1,4} \text{abs}\left(\frac{1}{\log(\mathbf{I}_i^H)}\right),$$

where $\mathbf{I}_i^H$ – the i-th element of the identified contour descriptor;

where $\mathbf{I}_i$ – the i-th element of the nominal contour descriptor.

Such a form of the formula for calculating the difference between descriptors was selected in order to use all the elements of descriptor vectors for distance calculation irrespective of their values. The block diagram of the algorithm described above is shown in Fig. 2.

Bench testing of the recognition algorithm

For testing the recognition algorithm, we developed a lab test bench comprising 10 IR diodes L-53SF6C (d=5 mm, 860 nm, 100 mW) arranged on a 0.5 × 0.5 m T-shaped pad.

Fig. 3 (left) shows the image sent from the IR camera to the recognition algorithm input; the right image illustrates the result of morphological closing operation applied to this image.

The completed operations allows to reliably separate the marker represented as IR markers from interference (the test bench uses daylight sources as interference).

Software-based simulation of the autonomous landing process

Within the scope of the study, we developed a software package for simulating UAV movement during landing. This software package is designed to analyse the algorithm accuracy and operation time depending on the automatic landing trajectory and initial data, i.e. recognition algorithm parameters, and allows to animate landing zone search and UAV descent.

Fig. 4 shows a frame resulting from animation of the target search and landing process. Letter a indicates the UAV position at the initial point of animation. The landing zone search stage takes

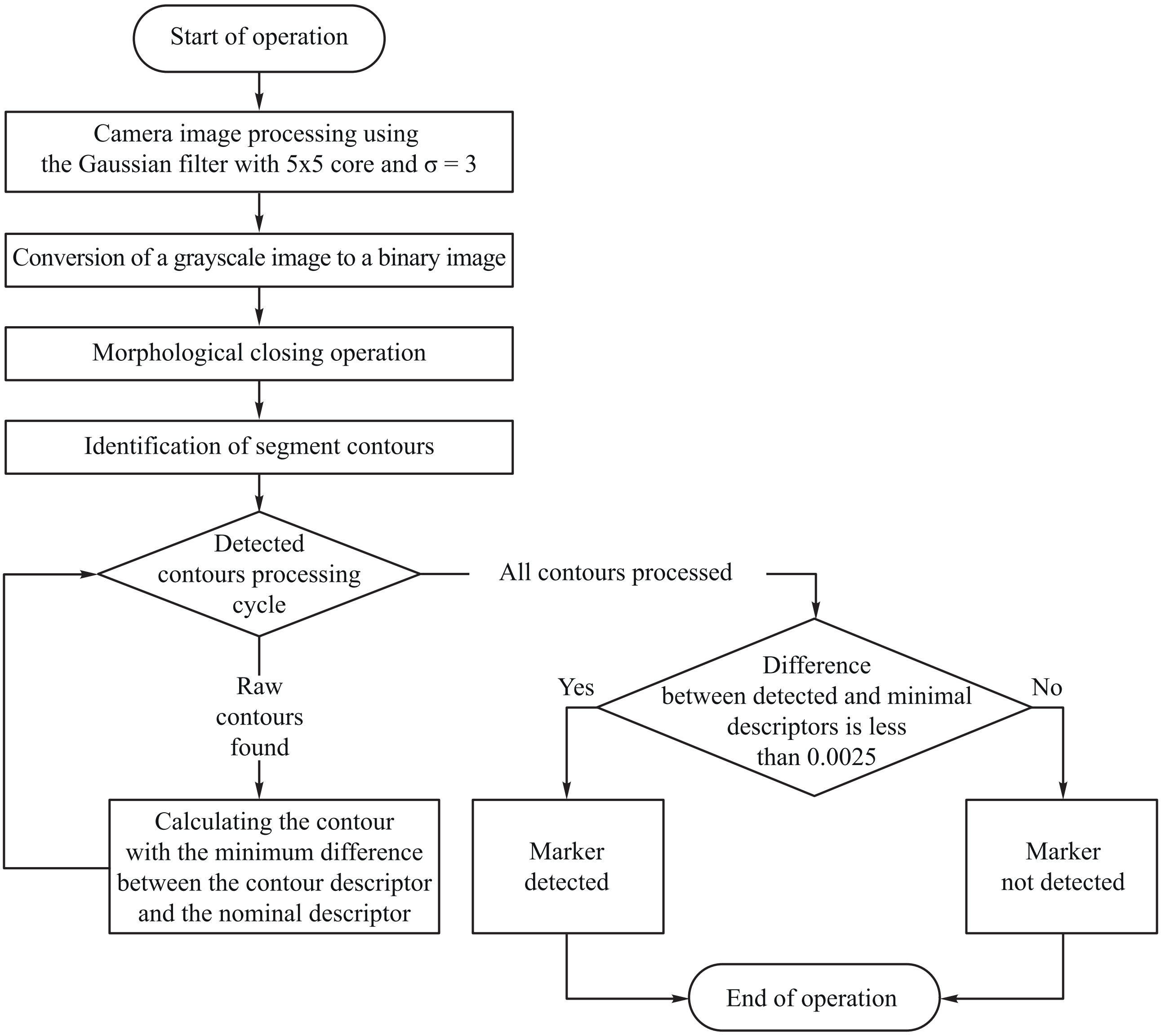

Fig. 2. Block diagram of recognition algorithm

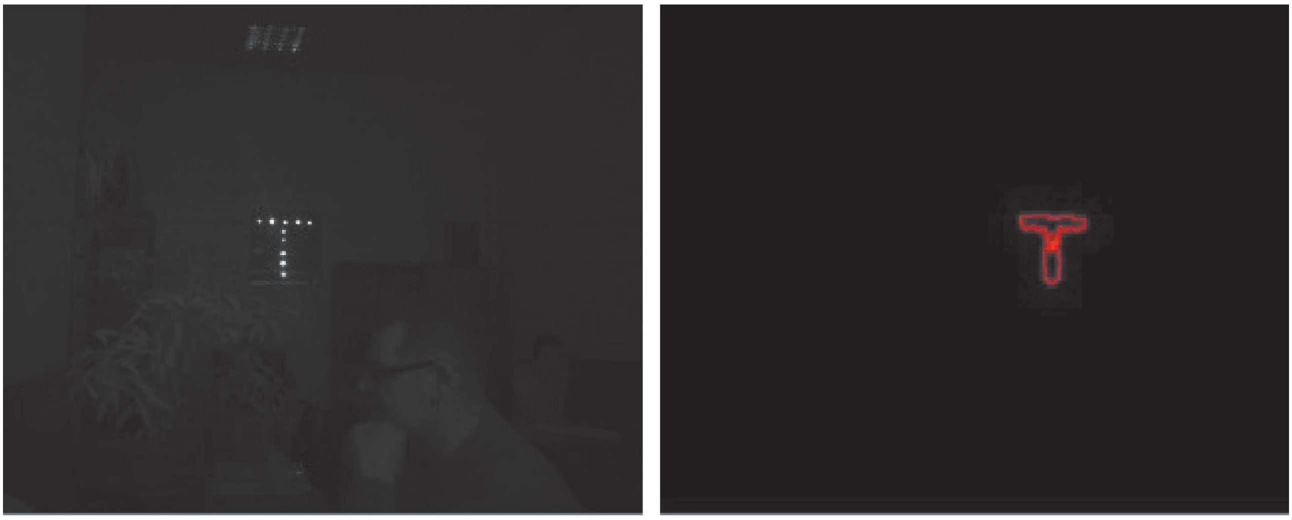

Fig. 3. Morphological closing for a structure made of IR diodes

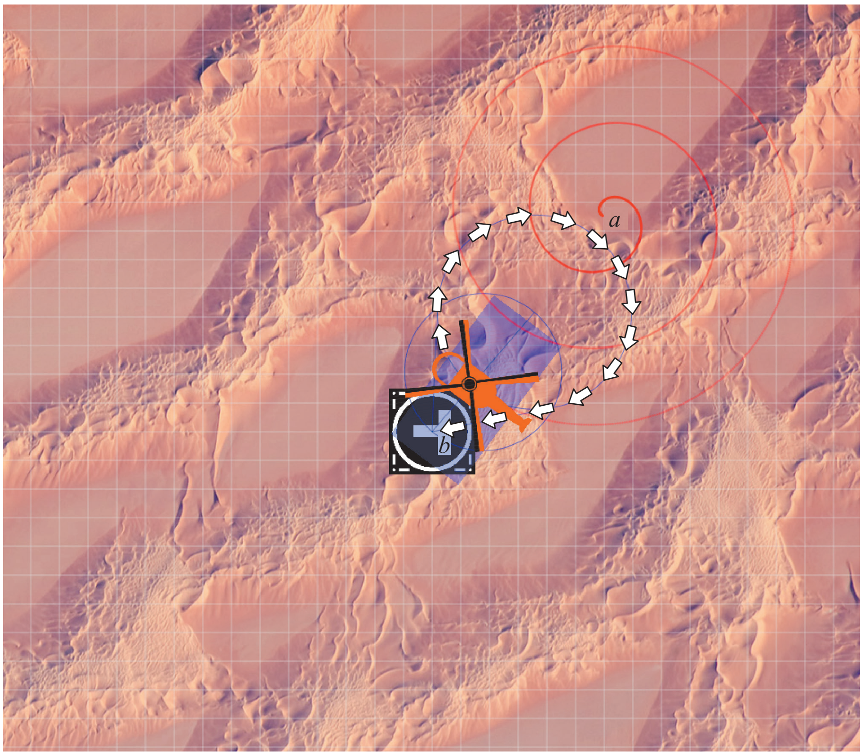

Fig. 4. Animation frame illustrating a helicopter-type UAV approaching the landing zone:
a – initial point; b – landing zone marker;
⇨ – landing trajectory

place as a UAV flies following the helical trajectory from the initial point to the current position. There is a violet rectangular area above the helicopter, which corresponds to the IR camera view area. Fig. 4 shows the frame where the IR camera detected landing zone marker *b*. A *T*-shaped contour was detected in the camera coverage area, and then the landing trajectory was calculated.

Fig. 5 shows graphs based on the approach simulation data. The approach was simulated using a computer with *Intel Core i*5 3.2 Ghz CPU.

The intersection of straight line *a* and the abscissa axis corresponds to the point where the landing zone marker position was identified, with the recognition error reaching the nearest to zero value for the first time. The gap between straight lines *b* and *c* corresponds to helicopter descent. Along with that, the helicopter is located above the landing zone while covering the remaining distance as shown in Fig. 5, where the difference between descriptors is minimal. In the segment following the intersection between straight line *c* and the abscissa axis, the *T* letter expands beyond the camera coverage, so the difference between descriptors increases.

Further development of the landing zone marker recognition algorithm

The next steps in development of the recognition algorithm are as follows:

• selection of industrial-type equipment for problem solving;

• full-scale testing of the existing algorithm and proving the correct choice of equipment;

• study of the feasibility of using a modulated IR radiation source as a landing zone marker;

• development and testing of the completed optical system on a small helicopter.

For now, we are planning to conduct full-scale tests of the developed recognition algorithm. The test objective is to select an IR camera and a landing zone marker, assuming that an IR camera will be placed at the distance of 100 m from a landing zone marker. Also, we need to select special-purpose equipment (for example, a single-board computer module)

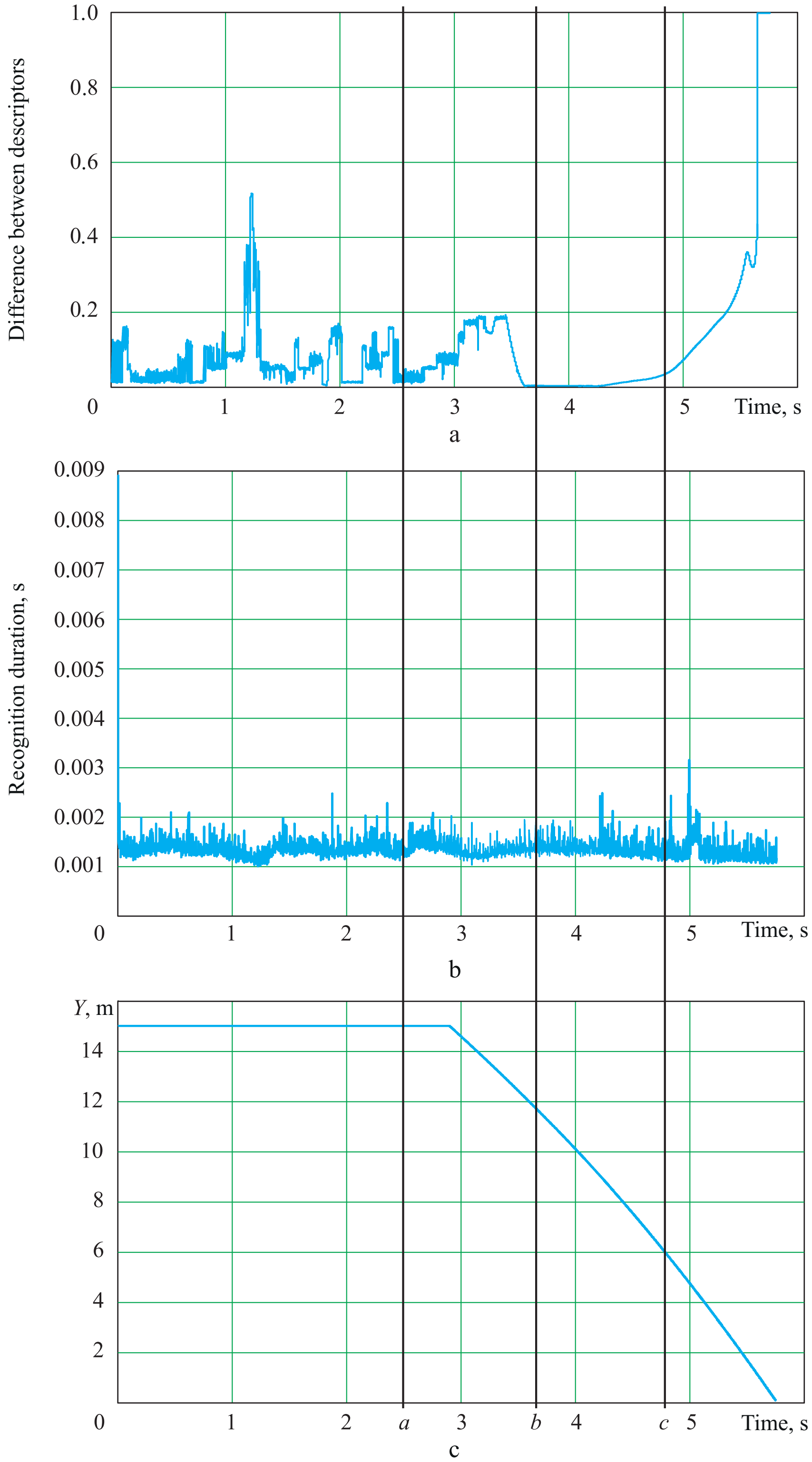

Fig. 5. Graphic representation of the UAV landing simulation result:
a – dependence of the difference between descriptors on time;
b – dependence of each frame recognition duration on time;
c – dependence of flight altitude along *Y*-axis on time

to be installed on a helicopter with certain problem-oriented characteristics.

In the future, the existing algorithm will be tested together with a selected helicopter airborne camera and equipment for indicating a landing zone marker.

We are interested in the study into the feasibility of using a modulated IR radiation as a landing zone marker, similar to the product developed by *IR-Lock* [6]. Since 2015, the company has launched commercial production of equipment sets including IR cameras and IR beacons with performance characteristics that make it possible to recognize objects in any weather conditions, in bright sunlight and at night. The in-house technology allows to avoid recognition errors and unwanted landings.

After all kinds of tests are completed and the final product is made, it is planned to test the product on a helicopter with the takeoff weight over 450 kg.

Bibliography

1. Research on computer vision-based for UAV autonomous landing on a ship / *G. Xu* et al. // Pattern Recognition Letters. 2009. No. 30. P. 600–605.

2. *Otsu N.* A threshold selection method from gray-level histograms // Proc. 1979 IEEE Trans. Sys. Man. Cybern. No. 9 (1). P. 62–66.

3. *Saripalli S., Montgomery J., Sukhatme G.* Vision-based autonomous landing of an unmanned aerial vehicle // Proc. 2002 IEEE Intern. Conf. on Robotics and Automation. P. 2799–2804.

4. *Gonzalez P., Woods R., Eddins S.* Digital Image Processing. [Transl. from Eng.] M.: Tekhnosfera, 2005.

5. *Flusser J., Suk T., Zitová B.* Moments and moment invariants in pattern recognition. Wiley & Sons Ltd., 2009. 312 p.

6. IR-LOCK. URL: http://irlock.com

Submitted on 23.11.2016

Ivannikov Konstantin Valerievich – Head of Department, Joint Stock Company State Research Institute of Instrument Engineering, Moscow.
Science research interests: unmanned aerial vehicle.

Gavrilov Aleksey Vladmirovich – Candidate of Engineering Sciences, leading software engineer, Joint Stock Company State Research Institute of Instrument Engineering, Moscow.
Science research interests: image recognition.

Boev Anton Sergeevich – software engineer, Joint Stock Company State Research Institute of Instrument Engineering, Moscow.
Science research interests: image recognition.

Shoshin Ilya Sergeevich – Software engineer, Joint Stock Company State Research Institute of Instrument Engineering, Moscow.
Science research interests: image recognition, 3D-modeling.

Способ посадки беспилотного летательного аппарата вертолетного типа с использованием инфракрасной камеры

Предложено использовать инфракрасную камеру для распознавания фигуры из набора инфракрасных излучателей – ориентиров на посадочной площадке. Построен и протестирован на стенде алгоритм распознавания инфракрасных ориентиров. Создан программный комплекс для моделирования распознавания посадочной площадки в процессе посадки беспилотного летательного аппарата (БПЛА) вертолетного типа.

Ключевые слова: посадка, БПЛА, вертолет, инфракрасная камера.

Иванников Константин Валерьевич – начальник отдела ОАО «ГосНИИП», г. Москва.
Область научных интересов: беспилотные летательные аппараты.

Гаврилов Алексей Владимирович – кандидат технических наук, ведущий инженер-программист ОАО «ГосНИИП», г. Москва.
Область научных интересов: распознавание образов.

Боев Антон Сергеевич – инженер-программист ОАО «ГосНИИП», г. Москва.
Область научных интересов: распознавание образов.

Шошин Илья Сергеевич – инженер-программист ОАО «ГосНИИП», г. Москва.
Область научных интересов: распознавание образов, 3D-моделирование.